https://doi.org/10.1590/jatm.v13.1202 ORIGINAL PAPER

The 6,500-H Life Test Results of 30 cm Diameter Ion Thruster

Sun Mingming[1,*], Geng Hai[1], Zheng Yi[1]

1. China Academy of Space Technology – Lanzhou Institute of Physics – Science and Technology on Vacuum Technology and Physics Laboratory – Lanzhou/Gansu – China
*Corresponding author: smmhappy@163.com

ABSTRACT

The life test of the 30 cm diameter ion thruster developed by the Lanzhou institute of physics began in Apr. 2018 and ended in Jan. 2020, lasting 6,500 h. This paper introduces the results of the 6,500-h life test of the 30 cm diameter ion thruster completed on the ground, including the ground facility for life test, the variations of the thrusters working performance, the times of the breakdown and power restart, and the erosion of the key components. The results show that the performance parameters, such as thrust, specific impulse and efficiency, do not change obviously during the test and magnetic field of the discharge chamber has no change. With the increase of test time, breakdown times increased significantly, whereas the power restart time decreased correspondingly. The diameter of the cathode orifice decreases gradually and there is a blockage risk of orifice. However, the diameter of the keeper orifice increases and presents an inverted cone erosion pattern. The diameter of the decelerator grid aperture expanded from 1.6 to 1.8 mm from 0 to 1,000 h and slightly enlarged after that. The aperture diameter of the accelerator grid presented linear enlargement but the pits-and-grooves erosion is obvious.

Keywords: Thruster; Life test; Performance; Erision; Grid gap.

INTRODUCTION

Ion thrusters (Chien *et al.* 2006; Brophy 2002; Goebel *et al.* 2002) have received a lot of attention in recent years due to high specific impulse (from 2,000 to 10,000 s) and the highest work efficiency (from 60 to 80%) compared to the conventional chemical propulsion system. These thrusters have many possible uses in both satellite station-keeping and deep-space prime propulsion. In 2012, the Lanzhou institute of physics (LIP) developed a 20 cm diameter ion thruster that can generate 40 mN of thrust with a specific impulse of 3,000 s. In October of this year, LIP carried out the first flight demonstration and verification of China's electric propulsion system by ShiJian-9A (SJ-9A) satellite (Chen *et al.* 2016; Tianping *et al.* 2013). The ion thruster has been working in orbit for hundreds of hours so far. In 2014, for the application demand of China's new generation of the large-scale truss-type satellite platform, a 30 cm diameter ion thruster was designed for the platform (Sun *et al.* 2018a; Sun *et al.* 2020a), which can generate 100 and 200 mN of thrust, respectively, in 3- and 5-kW operation modes. The specific impulse of these two modes is 3900 and 3500 s, respectively. The 30 cm diameter ion thruster successfully entered orbit with ShiJian-20 (SJ-20) satellite in October

Received: Sep. 7, 2020 | **Accepted:** Nov. 24, 2020.
Peer Review History: Double-blind Peer Review.
Section Editor: T. John Tharakan

2019 after the failed launch of the XinYan-4 (XY-4) satellite in 2017. In-orbit work verification started in May 2020, which has completed a total of 60 h of work time by Jun. 2020. At present, all in-orbit verification work of the thruster has been completed and the performance parameters meet the criteria. The thruster will implement satellite station keeping and orbit transfer in the future. The ground life test and verification of the 30 cm diameter ion thruster started in Apr. 2018 and ended in Jan. 2020. The test has completed 15 sections, with a total time of 6,500 h. Meanwhile, this is the first time for China to perform a life test of high power 30 cm diameter ion thruster.

Some research institutions have carried out life test on ion thrusters. In the 8,200-h life test of the NASA Solar Electric Propulsion Technology Application Readiness (NSTAR) ion thruster (Polk *et al*. 1999), serious corrosion appeared in the screen grid in the first 2,000 h and there were sputterings in the discharge chamber. After reducing the grids gap, there is almost no corrosion of the screen grid, however, the accelerator grid has an obvious corrosion, which is the main factor to influence the thruster life. The breakdown frequency in the early work stage (about seven times per hour, 0 ~ 800 h) is much higher than that in the subsequent work stage (once per hour) and the breakdown occurred mainly at the center area of the grids. According to XIPS-13 ion thruster life test in 2005 (Chien *et al*. 2005), the life test results show that in the performance parameters, such as thrust and specific impulse, exist a degradation of 1.2 and 0.5%, respectively. The thruster functional failure for the severe ion erosion of the grids after 16,146 h accumulated working time and the center line misalignment of the screen and accelerator grids are the main reason causing the grids erosion. In the 18,000-h life test of u-10 ion thruster (Hayashi 1983), the erosion of the grids aperture presents a nonlinear increase in the first 1,000 h and it presents an obvious monotone, increasing with the test time after 1,000 h. The 5,000 h endurance test results of RIT-22 ion thruster (Leiter *et al*. 2007) show that the inflection point of the accelerator grid aperture curve with test time appears at 1,200 h. The erosion of the aperture presents an exponential increase in 0 ~ 1,200 h and the average erosion velocity is about 3.2×10^{-3}mm/100 h. In contrast, the increase of aperture erosion becomes linear after 1,200 h and the average erosion velocity is 1.1×10^{-3} mm/100 h. These test results of the ion thrusters have well formulated the different phenomena during tests and the design defects and performance variation characteristics of ion thruster, as well as the life influencing factors, can only be verified by ground life test.

According to the operation requirement of the SJ-20 satellite, the in-orbit working life of the 30 cm diameter ion thruster is required to reach up to 20,000 h. Therefore, it is necessary for the thruster to carry out a lifetime verification test in the ground environment. The ground test results, such as thrust, specific impulse and the erosion of the key components, which can be used to prove whether performance and lifetime of the thruster, can meet the in-orbit requirements of the satellite. This paper introduces the ground test equipment and the results of the first 6,500 h life test of the 30 cm diameter ion thruster, including the thruster performance parameters, breakdown numbers, power restart times and corrosion of key components in each test section. The reasons leading to the variation of breakdown and power restart times are analyzed. In addition, the erosion of the cathode and the grids are also investigated.

EQUIPMENT AND TEST SECTIONS

As shown in Fig. 1(a), the 30 cm diameter ion thruster adopts four ring permanent magnets to form a ring-cusp magnetic field configuration. In order to reduce the sputtering corrosion effect of ions on the accelerator grid, a decelerator grid is added on the traditional two grids design (the screen and accelerator grids) to form a triple grid assembly to extend the working life of the accelerator grid (Fedorov *et al*. 2017). Since the transparency of the grids has a direct influence on the discharge loss and mass utilization efficiency, the grid is machined with many small apertures. High ion transparency and neutral transparency drives the grid design toward larger screen grid apertures and smaller accelerator grid apertures. Meanwhile, the aperture radius of the decelerator grid is slightly larger than that of the accelerator grid. The aperture radius of the screen grid, the accelerator grid and the decelerator are 0.95, 0.55 and 0.65 mm, respectively. A hollow cathode with the emission current of 20 A is installed in the discharge chamber, while a hollow cathode with the emission current of 5 A is used as a neutralizer. During the thruster operation, the gas flow rate of the anode is 48 sccm and the anode voltage is in the range of 30 to 34 V.

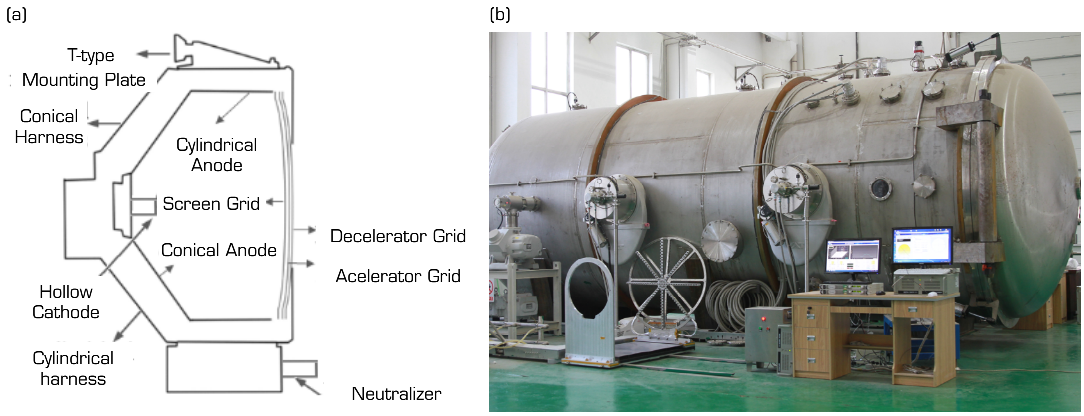

Figure 1. (a) Schematic of the 30 cm diameter ion thruster. (b) Vacuum facility for electric propulsion ground life test.

Figure 1(b) depicts the large vacuum facility specifically designed for ground test of the 30 cm diameter ion thruster. The facility is divided into two parts, an accessory chamber and main chamber. The ion thruster is mounted inside the accessory chamber to ensure that the plume can fully extend and the facility maintains a certain vacuum degree by the main pumping system. A sputtering target is installed at the end of the main chamber to prevent high-energy particles from directly colliding with the wall. The accessory chamber is 2m in length with diameter of 2m and the main chamber is 10m in length with diameter of 4.5m. The ion thruster is installed along the centerline of the accessory chamber and the grid surface is aligned with the chamber. Six cryogenic pumps are mounted at equal intervals on both sides of the facility, which have a total pumping speed of 260 kL/s. They provide a base pressure of 1×10^{-4} Pa, with the 30 cm diameter thruster full power flow rates. A shutter shaped titanium sputtering target with 18 blades is mounted at the end of the main chamber and liquid nitrogen pipeline is welded on the sputtering target. During the experiment, various sensors were installed to monitor the variation of the temperature, beam current and vacuum degree.

The life test is comprised of several sections, each has a different duration, and the thruster working mode also differs in each section of the test. The life test of the 30 cm diameter ion thruster is divided into 15 sections. Sections 1 to 9 (0 ~ 3,600 h) is mainly to verify the thruster performance in 3 kW operating mode. In the later stage of the test, namely sections 10 to 13 (3,600 ~ 5,500 h), the thruster performance under 5 kW operating mode is mainly verified. The arrangement of test time depends mainly on the requirements of the satellite in-orbit operation (Lai *et al.* 2016), also determined by requirements of the research on the erosion of the thruster under different operating modes.

The thruster on/off verification is carried out mainly in the middle and late stages of life test, namely the 5-kW operating mode. This is due to the higher risk of breakdown when the thruster started directly from cold state in high power work mode. The high-power mode causes the thruster to generate more heat in a short period of time. Meanwhile, the heat causes greater thermal deformation of the grid assembly, which will increase the risk of breakdown between the grids.

THE PERFORMANCE VARIATION

The performance of the thruster, such as thrust, specific impulse and efficiency, was monitored during the lifetime test. As shown from Fig. 2(a) to 2(d), the variation range of power, thrust, specific impulse and efficiency under 3 kW operating condition is 2,720 ~ 2,850 W, 98 ~ 102 mN, 3,800 ~ 3,920 s and 67 ~ 70%, respectively. The variation range of power, thrust, specific impulse and efficiency under 5 kW operating condition is 5,060 ~ 5,240 W, 198 ~ 205 mN, 3,450 ~ 3,510 s and 65 ~ 68%, respectively.

As detailed in Fig. 3(a), the magnetic field was measured in different test sections and magnetic field intensity of five points A ~ E were measured by magnetometer. Twelve sets of data were measured in each point at an interval of 30° around the axis of the thruster and the average value was taken to obtain the changes in magnetic field intensity at different positions of the discharge chamber, which is shown in Fig. 3(b).

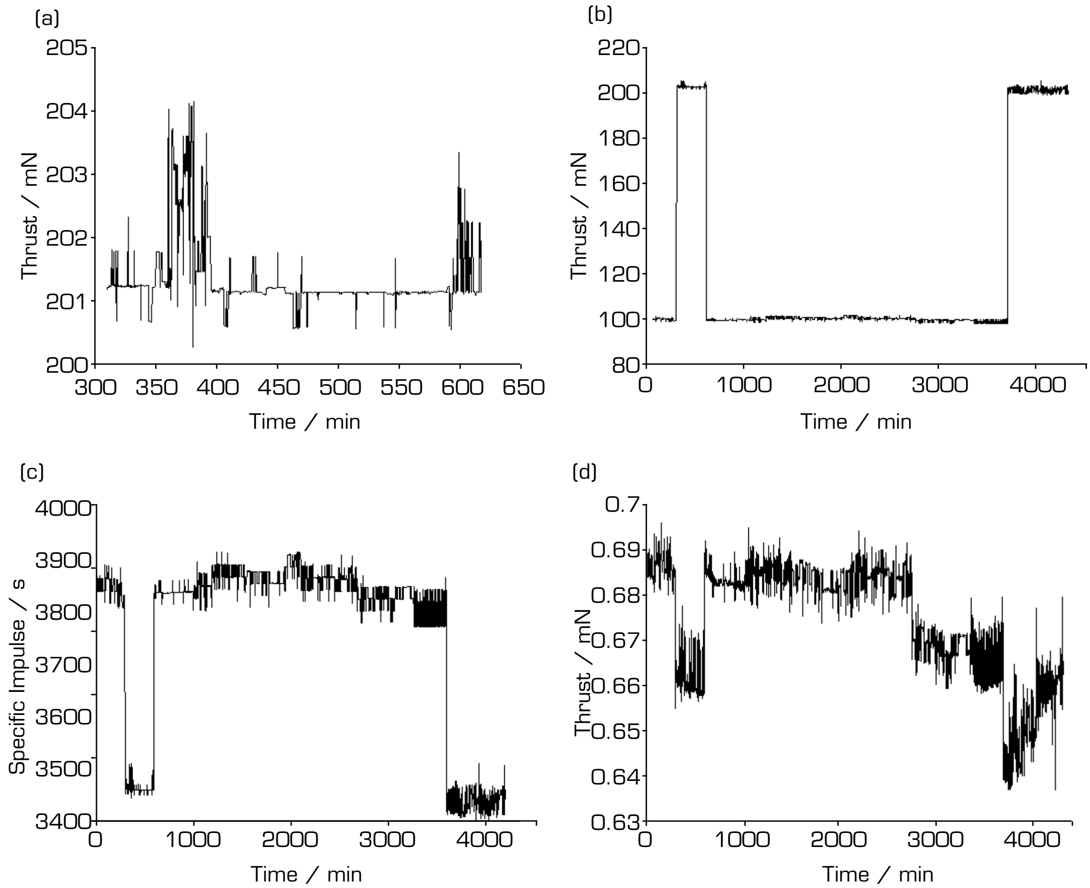

Figure 2. Performance variation of 30 cm diameter ion thruster in the life test. (a) Thrust (300 ~ 650 h); (b) Thrust (0 ~ 4500 h); (c) Specific Impulse (0 ~ 4,500 h) and (d) Efficiency (0 ~ 4,500 h).

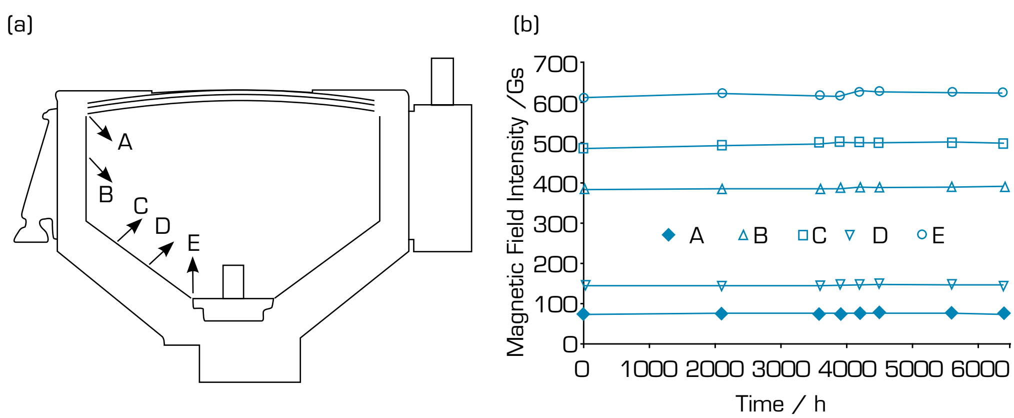

Figure 3. Magnetic field measure position (a) and intensity test results (b).

Figure 3(b) shows that the magnetic field intensity is stronger when closer to the magnetic pole and the average magnetic field intensity at different positions of the discharge chamber did not change significantly in the 6,500-h life test. The test result means that the permanent magnets currently used in the discharge chamber can tolerate varying temperatures during operation and the magnetic fields are almost unaffected by the temperature change.

THE BREAKDOWN TIMES

The breakdown of the thruster means that when the grids gap thermal spacing is too small (Sun *et al.* 2018b), or when the tiny sputtering materials from discharge chamber or the grids are diffused by the plume, moving to the screen grid and the accelerator grid or the accelerator grid and the decelerator grid, resulting in instantaneous short-circuit of the power supply. The sputtering materials will be instantly melted by the high current generated by the short circuit and the grids gap is restored to the pre-breakdown spacing after the amount of energy released at the moment of breakdown. Therefore, the breakdown lasts only a short period of time and generally in the order of tens of microseconds, which can only be monitored through oscilloscope. In addition, most of the breakdowns are transient (the last time is too short to trigger the protection of the power), while only a long duration of breakdown (this may be due to larger metal sputterings or contact between the grids) will cause the power restart. Therefore, not all breakdowns cause power restart and the number of power restart is not included in the number of breakdowns. The breakdown frequency is one of the most important indexes to evaluate the performance of the thruster (Goebel and Schneider 2005; Goebel 2005). When the breakdown frequency increases, it indicates that the sputtering produced in the discharge chamber increases. The reason for this phenomenon is that the discharge loss of the thruster increases and more high-energy ions are produced, which leads to the increase of sputtering. For the 30 cm diameter ion thruster, the breakdown occurs when the current of screen grid and the accelerator grid are larger than 4.8 and 2.1 A in 5 kW work mode, respectively, and are larger than 3.2 and 1.2 A in 3 kW work mode, respectively. At the same time, a breakdown protection process for the PPU (power process unit) was formulated. When the breakdown is detected, the control unit starts the timer. Within 2 s after the breakdown, the control unit does not restart the power protection, but only records the last time of the breakdown and the hardware implements the automatic power recovery. In the following 2.5 s, when the control unit detects a breakdown, it will immediately implement the power restart protection. The protection process is to turn off the power supply of the screen grid and the accelerator grid, and reduce the anode current to 7.5 (3 kW work mode) or 10 A (5 kW work mode). Power is restored after 10 s and automatically shuts down if the power is restarted more than 6 times before the ion beam reaches the rating. Figure 4(a) shows the cumulative breakdown times of each test section, that is, the total number of breakdowns within a specified time period and the power restart times of each test section is shown in Fig. 4(b).

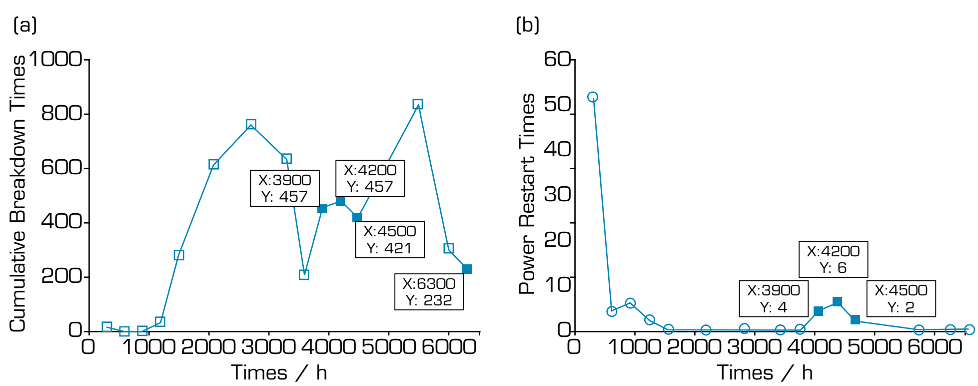

Figure 4. Cumulative times of breakdown (a) and power restart (b) in the test.

As seen from Fig. 4(a), the cumulative breakdown times in the first three test sections (0 – 1,200 h) is very small, which can even be ignored. However, the power restart times corresponding to this period, shown in Fig. 4(b), is much higher than other test sections. It is estimated that the main reason for this phenomenon is that, at the initial stage of the test, the edges and corners of the thrusters are etched rapidly by ions and some large sputter are generated. The sputter thereby drifts to the middle of the grids under the interaction of the internal fluid movement in the discharge chamber, resulting in the short circuit of the power supply and the restart of the power. With the increase of the test time, when the edges and corners of ion thruster are etched by ions, it will not produce larger sputters, on the contrary, a large number of small sputters are generated. Therefore, as shown in

Fig. 4(a) and 4(b), the power restart times in 1,200 – 6,500 h decreased to less than 10 times and cumulative breakdown times in 1,200 – 6,500 h increased significantly than 0 – 1,200 h. Meanwhile, it is found that the power restart times in 5 kW work mode [3,900, 4,200 and 4,500 h in Fig. 4(b)] is higher than 3 kW work mode, which means high power work mode will generate larger sputter to enhance the power restart chance than low work mode. However, as shown in Fig. 4(a), the probability of producing smaller sputters is almost the same in the 3- and 5-kW working mode.

THE EROSION OF KEY COMPONENTS

The hollow cathode and the grids are significantly affected by ion erosion during the life test of the ion thruster. For the hollow cathode, the main concern is an early failure, structural wear and performance changes. These factors finally infer the risk and probability that the hollow cathode may lead to a failure of the thruster. The main wear parts of the hollow cathode are the keeper and the orifice (Goebel *et al*. 2005). The erosion of the keeper will lead to the heater being exposed to the plasma environment in the discharge chamber (Kolasinski and Polk 2003; Domonkos *et al*. 2005). The erosion of the orifice will cause the electrons not to be extracted from it.

Figure 5(a) describes the erosion depth of the thickness of the keeper and variation of the radius of the cathode orifice, which indicates that the thickness of the keeper is reduced from 1.2 to 0.95 mm and the radius of the cathode orifice from 0.81 to 0.76 mm in 1,200 to 6,500 h, respectively. In the early stage (1,200 – 4,200 h), the cathode orifice shrank linearly and slowly, whereas the erosion depth of the keeper increased rapidly. After that, the erosion depth gradually decreased. The main reason for this phenomenon is that the erosion of the keeper is centered on the keeper orifice, showing a corrosion characteristic of an expanding inverted cone so that the thickness of the keeper changes little in the later stage of the test. Figure 5(b) shows the radius erosion of the keeper orifice, which has a similar phenomenon and reason to the erosion depth of the keeper. According to the test results, the radius of the keeper enlarged significantly in the early 3,000 h, from 1.35 to 1.45 mm and, after that, the expansion speed of the keeper orifice gradually lowers. The distance between the cathode orifice plate and the keeper has the characteristic of monotonic decreasing, which is mainly due to the designed structure of the cathode and the thermal deformation caused by the high temperature when the cathode works.

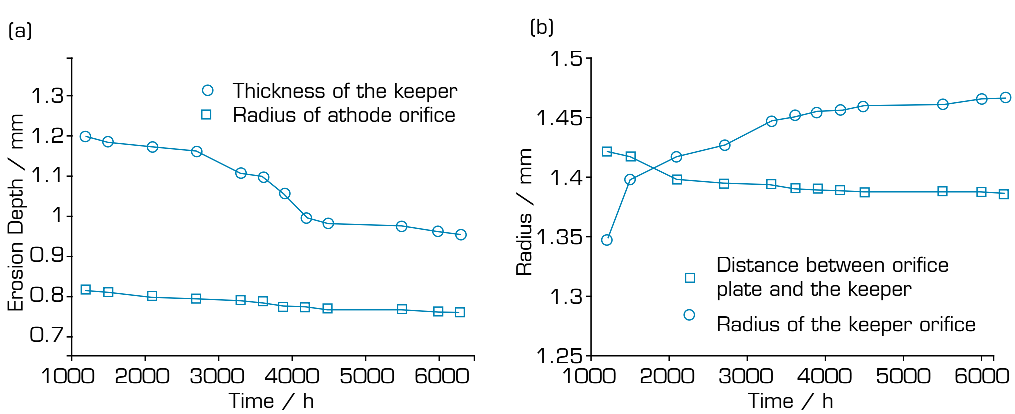

Figure 5. Erosion depth (a) and diameter variation (b) of the keeper and the orifice.

Figure 6 show the erosion of the cathode orifice in 1,200, 3,600 and 6,400 h, and the corresponding erosion trend. The cathode orifice is corroded from a circle into an irregular circle and a large number of protrusions appeared on the edge of the orifice, which is mainly caused by ion sputtering and the deposition of the sputter on the wall of the orifice under the high temperature. As test time increases, there is a risk that the hollow cathode orifice will be blocked by the sputters and will not emit electrons.

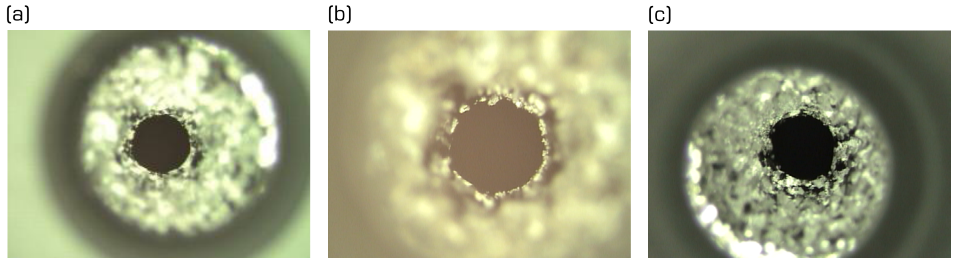

Figure 6. Erosion of the cathode orifice (a) 1200 h; (b) 3600h and (c) 6400h.

The erosion of the keeper orifice in 1,200, 4,500 and 6,400 h is presented in Fig. 7(a) - (c). According to the test results, the keeper orifice radius of 4,500 h enlarged from 1.35 to 1.45 mm compared to the 1,200-h orifice radius, and that of 6,400 h only enlarged from 1.45 to 1.48 mm. During the 6,500-h life test, the shape of the keeper orifice remained a regular circle, but the wall of the keeper orifice presented an inverted conical shape with the outlet larger than the inlet due to the ion erosion effect. In addition, the edge of the keeper orifice is rough because of the effect of ion sputtering.

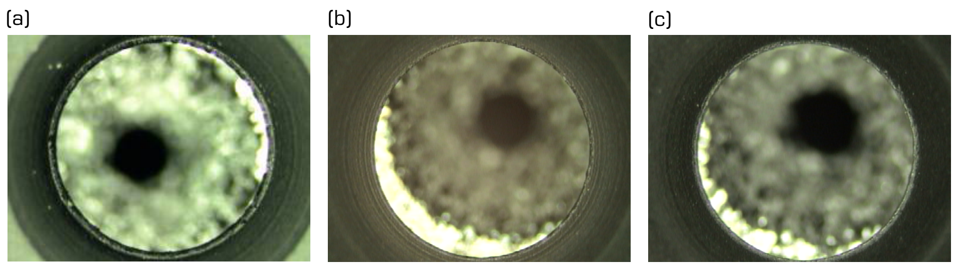

Figure 7. Erosion of the keeper orifice (a) 1200 h; (b) 3600h and (c) 6400h.

The grid gap variation and the aperture erosion of the grids are also investigated during the life test. The gap variation and aperture erosion in different regions of the grids are all measured by three-dimensional profilometer, which can obtain discrete position the edge points of aperture, and the radius variation of aperture is obtained by fitting the position data of the edge points. The test area of the grids is divided into 12 marginal regions (spaced at equal intervals of 30 degrees) and a central region. Each measurement area is a circular area with a diameter of 5 cm and the gap variation is measured a total of ten times and the average value is taken. The ion beam density and the temperature at the center of the grids are the highest (Sun *et al*. 2020b). Therefore, the variation of the grids gap in the central area of the grids is also the largest. This paper will only focus on this gap.

Figure 8(a) shows the grids gap variation in the life test of the ion thruster, which indicates that the gap between the screen grid and the accelerator grid increased from 0.83 to 1.1 mm. In the first 300 h, the grid gap increased rapidly from 0.83 to 0.98 mm, an increase of about 19%. Over the next 300 to 6,500 h, the grid gap increases slowly and linearly. The gap between the accelerator and the decelerator grids have the same variation trend, which indicates the grid gap increased rapidly from 0.61 to 0.65 mm in the first 300 h and, after this, the grid gap has change little. The reason for the variation trend of the grid gap is that, in the first 300 h, the grid material begins to have thermoplastic deformation and the deformation is the largest. Due to the kinematic hardening characteristic of the strain of molybdenum material, the plastic strain of the material gradually decreases in the subsequent temperature cycle.

Figure 8(b) illustrates the diameter variation of the apertures in central area of the decelerator and accelerator grids. The results indicate that the erosion of the decelerator grid is significant within 0 – 1,200 h; however, after 1,200 h, the enlargement of aperture is not notable. This is mainly triggered by the fact that the decelerator grid is in the outermost layer of the grids assembly. In the initial assembly, the center of the grid apertures is not ensured to be completely aligned and the grid gap will change greatly during the working process, so that the focusing of the ion beam will also change. Therefore, in the early stage of thruster life test, the ion beam will directly bombard the decelerator grid aperture with poor focusing performance, resulting in a rapid erosion speed and distinct irregular circle of the grid aperture.

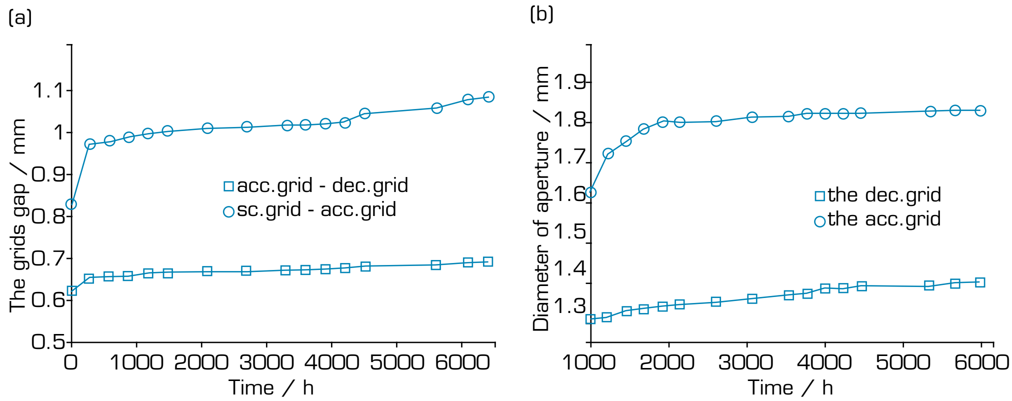

Figure 8. Variation of the gap (a) and diameter (b) of the grids.

The irregular shape caused by ion erosion will remain stable in the later stages of the life test. This phenomenon is more obvious in the edge of the decelerator grid (due to thermal deformation effect, the grid aperture in the edge region has the greatest center aligned change) and a part of the apertures at the edge of grid are corroded and appear to be elliptical or hexagonal stars. However, after the center aligned change of the edge of the grid is etched, there is little etching. The accelerator grid aperture is mainly bombarded by charge exchange xenon (CEX) ions instead of the beam and what causes the final failure mode of the thruster is the electron back-streaming failure (Williams *et al.* 2003). The screen grid is located in the innermost layer of the grids assembly and the probability of ions directly bombarding the screen grid is very low, the enlargement of the screen grid aperture is very small and almost unchanged during the whole test process.

Figure 9 shows the erosion of grid apertures in the central area of the accelerator grid, where pa distinct pits-and-grooves erosion pattern appears. In addition, the depth of the ring of erosion around the aperture (the grooves) is more obvious than pits shaped erosion between the apertures and this phenomenon is very similar to that of NSTAR and XIPS (Sengupta *et al.* 2003; 2004) ion thruster life test results. Pits-and-grooves erosion is caused by CEX ions and these ions striking the downstream surface of the accelerator grid can come from several centimeters downstream of the grid, the discharge near-field region. The density of CEX ions in the center of near-field region is the highest in ion beam, leading to the most severe erosion in the central region of the accelerator grid.

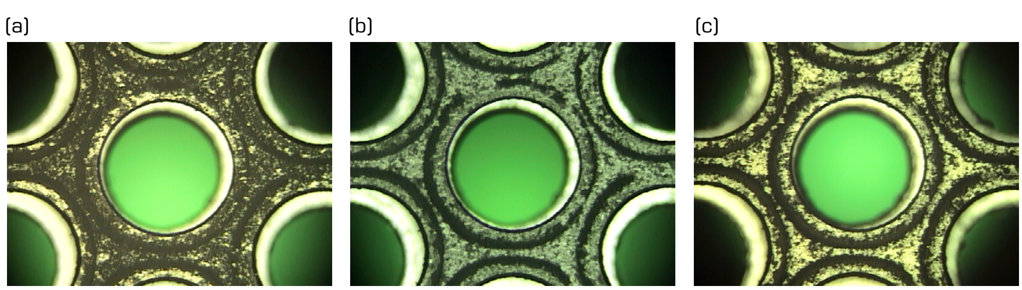

Figure 9. The grid apertures erosion in central area of the accelerator grid (a) 3300 h; (b) 4500h and (c) 6400h.

The erosion phenomenon and reasons of the decelerator grid and the accelerator grid in the early stage of life test are completely different. However, after the early stage of the test, the erosion of both the decelerator grid and the accelerator grid is determined by CEX. With the increase of test time, the pits-and-grooves erosion caused by CEX ions on the decelerator grid surface will lead to the first fall off and structural failure of the decelerator grid and this is exactly the purpose of the design of the decelerator grid (Wirz *et al.* 2007). The accelerator grid is shielded by the decelerator grid, which has no influence on the extraction of ion beam, but is used to reduce the number of CEX ions bombardment to the surface of the accelerator grid and extend the lifetime of the accelerator grid.

CONCLUSIONS

At present, the 30 cm diameter ion thruster developed by LIP has completed 15 sections, with a total life of 6,500 h, which will continue in the future. According to the results of the 6,500-h test, the performance parameters of the thruster, such as thrust, specific impulse and efficiency, do not change significantly.

The magnetic field intensity measured in the thruster discharge chamber after 2,100 h showed that the magnetic field has not changed, which indicated that the permanent magnet currently used in the thruster could withstand the high temperature generated by the thruster. The statistical results of the breakdown and the power restart times show that the breakdown times from 0 to 1,200 h are less than 50 times and the power restart times are more (which is caused by the large sputtering material produced from discharge chamber and the grids in the early stage of the test). With the increase of test time, smaller size sputtering materials are generated and lead to a significant increase in the number of breakdowns, while the power restart times decreases correspondingly. Moreover, the power restarts in 5 kW high power mode are more likely to occur than those in 3 kW low power mode. The radius of the cathode orifice decreases gradually due to the deposition of the sputter on the surface of the orifice wall and the keeper orifice presents an inverted cone due to the constant erosion of ions.

During 0 to 600 h of the test, both the gap between the accelerator grid and the decelerator grid, and the screen grid and the accelerator grid are increased and stabilized at 1.1 and 0.7 mm, respectively, in the early stage of the test due to the kinematic hardening of the strain of the material. Meanwhile, the diameter of the decelerator grid aperture rapidly expanded from 1.6 to 1.8 mm within 0 to 1,000 h, after which the erosion velocity is significantly reduced. The aperture of the accelerator grid shows a slow linear expansion trend; however, the pits-and-grooves erosion is obvious. During the whole life test, the corrosion of the screen grid is very low and the radius of the aperture is almost unchanged.

AUTHOR'S CONTRIBUTION

Conceptualization: Sun M M; **Methodology:** Sun M M; **Investigation:** Sun M M and Zheng Y; **Writing – Original Draft:** Sun M M; **Writing – Review and Editing:** Sun M M and Zheng Y; **Funding Acquisition:** Sun M M; **Resources:** Geng H; **Supervision:** Sun M M.

DATA AVAILABILITY STATEMENT

Data will be available upon request.

FUNDING

National Natural Science Foundation of China
http://dx.doi.org/10.13039/501100001809
Grant Nº: 61901202

ACKNOWLEDGEMENTS

The authors are thankful to Science and Technology on Vacuum Technology and Physics Laboratory for providing the test data.

REFERENCES

Brophy JB (2002) NASA's Deep Space 1 ion engine (plenary). Rev Sci Instrum 73(2):1071-1078. https://doi.org/10.1063/1.1432470

Chen J, Zhang T, Geng H, Jia Y, Meng W, Wu X, Sun A (2016) Analysis of Numerical Simulation Results of LIPS-200 Lifetime Experiments. Plasma Sci Technol 18:611. https://doi.org/10.1088/1009-0630/18/6/06

Chien K-R, Hart SL, Tighe WG, Pano MK, Bond TA, Spears R (2005) L-3 Communications ETI Electric Propulsion Overview. Paper presented 29th International Electric Propulsion Conference. IEPC; Princeton, New Jersey, United States. [accessed Jan 12 2020]. http://electricrocket.org/IEPC/315.pdf

Chien K-R, Tighe WG, Bond TA, Spears R (2006) An Overview of Electric Propulsion at L-3 Communications Electron Technologies Inc. Paper presented 42nd AIAA/ASME/SAE/ASEE Joint Propulsion Conference & Exhibit. AIAA; Sacramento, California, United States. https://doi.org/10.2514/6.2006-4322

Domonkos DT, Foster JE, Soulas GS (2005) Wear Testing and Analysis of Ion Engine Discharge Cathode Keeper. J Propuls Power 21(1):102-110. https://doi.org/10.2514/1.4441

Fedorov VA, Mogulkin AI, Obukhov VA, Abgaryan VK, Balashov VV (2017) Numerical Simulation of Temperature Deformation for Radio Frequency Ion Thruster Electrodes. Procedia Eng 185:24-30. https://doi.org/10.1016/j.proeng.2017.03.286

Goebel DM, Martinez-Lavin M, Bond TA, King AM (2002) Performance of XIPS Electric Propulsion in On-orbit Station Keeping of the Boeing 702 Spacecraft. Paper presented 38th AIAA/ASME/SAE/ASEE Joint Propulsion Conference & Exhibit. Indianapolis, Indiana, United States. https://doi.org/10.2514/6.2002-4348

Goebel DM (2005) High Voltage Breakdown Limits in Ion Thrusters Paper presented 41th AIAA/ASME/SAE/ASEE Joint Propulsion Conference & Exhibit. AIAA; Tucson, Arizona, United States. https://doi.org/10.2514/6.2005-4257

Goebel DM, Schneider AC (2005) High-Voltage breakdown and conditioning of carbon and molybdenum electrodes. IEEE Trans Plasma Sci 33(4):1136-1148. https://doi.org/10.1109/TPS.2005.852410

Goebel DM, Jameson K, Katz I, Mikellides I, Polk JE (2005) Energetic Ion Production and Keeper Erosion in Hollow Cathode Discharges. Paper presented 29th International Electric Propulsion Conference; IEPC; Princeton, New Jersey, United States.

Hayashi M (1983) Determination of electron-xenon total excitation cross-sections, from threshold to 100 eV, from experimental values of Townsend's α. J Phys D: Appl Phys 16(4):581. https://doi.org/10.1088/0022-3727/16/4/018

Kolasinski RD, Polk JE (2003) Characterization of Cathode Keeper Wear by Surface Layer Activation. Paper presented 39th AIAA/ASME/SAE/ASEE Joint Propulsion Conference and Exhibit. AIAA; Huntsville, Alabama, United States. [accessed Mar 20 2020]. https://trs.jpl.nasa.gov/bitstream/handle/2014/39126/03-1913.pdf?sequence=1&isAllowed=y

Lai CQ, Gu Z, Song YY, *et al.* (2016) Analysis of Spacecraft payload capacity based on ion propulsion system. Journal of Propulsion Technology 10(10):2183-2189. https://doi.org/10.13675/j.cnki.tjjs.180685

Leiter H, Kukies R, Killinger R, Bonelli A, Scaranzin S, Scortecci F, Neumann H, Tartz M (2007) RIT-22 Ion propulsion system: 5000h endurance test results and life prediction. Paper presented 43th AIAA/ASME/SAE/ASEE Joint Propulsion Conference & Exhibit, Cincinnati, Ohio, United States. https://doi.org/10.2514/6.2007-5198

Polk JE, Anderson JR, Brophy JR, Rawlin VK, Patterson MJ, Sovey J, Hamley J (1999) An overview of the results from and 8200 hour wear test of the NSTAR ion thruster. Paper presented 35th Joint Propulsion Conference and Exhibit. AIAA; Los Angles, California, United States. https://doi.org/10.2514/6.1999-2446

Sengupta A, Brophy J, Goodfellow K (2003) Status of the extended life test of the Deep Space 1 flight spare ion engine after 30,000 hours of operation. Paper presented 39th AIAA/ASME/SAE/ASEE Joint Propulsion Conference and Exhibit. AIAA; Huntsville, Alabama, United States. https://doi.org/10.2514/6.2003-4558

Sengupta A, Brophy J, Anderson J, Garner C, Banks B, Groh K (2004) An overview of the results from the 30,000 hr life test of Deep Space 1 flight spare ion engine. Paper presented 40th AIAA/ASME/SAE/ASEE Joint Propulsion Conference and Exhibit. AIAA; Fort Lauderdale, Florida, United States. https://doi.org/10.2514/6.2004-3608

Sun M, Wang L, Yang J, Wen X, Huang Y, Wang M (2018a) Study of the key factors affecting the triple grid lifetime of the LIPS-300 ion thruster. Plasma Sci Technol 20(4):045504. https://doi.org/10.1088/2058-6272/aaa66a

Sun M, Jia Y, Huang Y, Yang J, Wen X, Wang M (2018b) Study on the influence of three-grid assembly thermal deformation on breakdown times and an ion extraction process. Plasma Sci Technol 20:065509. https://doi.org/10.1088/2058-6272/aaad5d

Sun M, Zheng Y, Geng H (2020a) Grid gap variation of ion thruster during startup in orbit. IEEE Trans Plasma Sci 48(2):455-461. https://doi.org/10.1109/TPS.2020.2965798

Sun MM, Geng H, Long JF, Yang JT (2020b) Effects of different ambient temperature on ion erosion rate for triple grid of 30cm diameter ion thruster. Journal of Propulsion Technology 41(1):121-131. https://doi.org/10.13675/j.cnki.tjjs.2016.07.026

Tianping Z, *et al*. (2013) Initial flight test results of the LIPS-200 electric propulsion system on SJ-9A satellite. Paper presented 33rd International Electric Propulsion Conference. IEPC; Washington, DC, United States. [accessed Apr 10 2020]. http://electricrocket.org/IEPC/ewd4t7v4.pdf

Williams J, Goebel D, Wilbur P (2003) Analytical model of electron backstreaming for ion thrusters. Paper presented 39th AIAA/ASME/SAE/ASEE Joint Propulsion Conference and Exhibit. AIAA; Huntsville, Alabama, United States. https://doi.org/10.2514/6.2003-4560

Wirz RE, Anderson JR, Goebel D, Katz I (2007) XIPS Ion Thruster Grid Erosion Predictions for Deep Space Missions. Paper presented 30th International Electric Propulsion Conference. IEPC; Florence, Italy. [accessed Apr 15 2020]. http://electricrocket.org/IEPC/IEPC-2007-265.pdf